Environmental Science and Pollution Research (2025) 32:14020–14036
https://doi.org/10.1007/s11356-025-36512-2

RESEARCH ARTICLE

Assessment of the groundwater quality status of the phreatic aquifer in Grombalia (Tunisia) for irrigation via geostatistical modeling

Constantinos F. Panagiotou[1] · Thuraya Mellah[2,3] · Hatem Baccouche[2] · Marinos Eliades[1] · Lobna Mansouri[2] · Marinos Stylianou[4] · Nikolaos Stathopoulos[5] · Hanen Jarray[2] · Hanene Akrout[2]

Received: 26 April 2024 / Accepted: 5 May 2025 / Published online: 16 May 2025

Abstract

This study is the first attempt to characterize the suitability of the Grombalia phreatic aquifer for irrigation use by combining traditional classification diagrams with different geostatistical interpolation methods. The Wilcox and USSL diagrams suggest that only 20% of the groundwater samples satisfy the recommended sodium standards, whereas 50% of the groundwater samples are classified as unsuitable for irrigation because of salinity constraints. The spatial interpolation of four parameters, particularly electrical conductivity (EC), chemical oxygen demand (COD), chloride, and piezometric levels, is performed via ordinary kriging (OK). The results reveal the presence of high values of EC in the central and northern parts of the aquifer, and that chloride concentrations exceed the recommended irrigation standards in a large portion of the aquifer, mainly due to the presence of excessive industrial discharge. High levels of COD are observed in the northwestern part, probably due to anthropogenic sources. Indicator kriging (IK) revealed that a large portion of the northern part is likely to experience salinity and toxicity adversities, whereas the majority of the southern part is considered to be suitable for irrigation use. In particular, 38% of the study area is expected to be suitable for irrigation use concerning salinity (i.e., electrical conductivity and total dissolved solids (TDS)), whereas an even lower portion (16%) is expected with respect to chloride.

Keywords Irrigation suitability · Groundwater · Classification diagrams · Geostatistics · Tunisia

Introduction

Tunisia exhibits a diverse range of bioclimatic regions, covered by mountainous terrain in the northern part, North-Saharan steppe in the central area, and desert in the southern area. The northwestern areas experience an annual average rainfall of more than 1500 mm, whereas the southern region receives less than 100 mm annually (Henia 2008). Moreover, strong temporal variability in the precipitation rates has also been observed during the last half-century (Besbes et al. 2014).

Groundwater constitutes a major component of the water supply, particularly 44% of conventional water resources in Tunisia, and plays an essential role in the agricultural sector (Amwele et al. 2021). However, ensuring that groundwater quality is sufficient for use in agriculture is a challenging task because of the numerous potential sources of contamination that are present, such as urban run-off, domestic wastewater, and intensive use of fertilizers (Delbari et al. 2016; Khelifi et al. 2022; Panagiotou et al. 2022b).

Responsible Editor: Rongrong Wan

✉ Constantinos F. Panagiotou
constantinos.panagiotou@eratosthenes.org.cy

[1] Department of Resilient Society, ERATOSTHENES Centre of Excellence, Limassol, Cyprus

[2] Wastewater and Environment Laboratory, Water Research and Technologies Centre (CERTE), Borj Cedria, Tunisia

[3] Higher School of Digital Economy (ESEN), University of Manouba, Manouba, Tunisia

[4] Laboratory of Chemical Engineering and Engineering Sustainability, Faculty of Pure and Applied Sciences, Open University of Cyprus, Nicosia, Cyprus

[5] Operational Unit BEYOND "Centre for Earth Observation Research and Satellite Remote Sensing", Institute for Astronomy, Astrophysics, Space Applications and Remote Sensing, National Observatory of Athens, Athens, Greece

Previous studies revealed the presence of highly contaminated wastewater in the hydrological system near industrial complexes and large cities because the concentrations of water quality indicators exceed the recommended values (Taoufik et al. 2017; Gasmi et al. 2016). For example, water samples have been collected from different locations along the national river network, revealing the presence of high concentrations of salinity, chemical oxygen demand (COD), organic pollutants, biochemical oxygen demand (BOD), microbiological parameters, and heavy metals (Khadhar et al. 2013; Gasmi et al. 2016; Khouni et al. 2021). Furthermore, groundwater is experiencing a decline in both quantity and quality due to climate change, extended drought conditions, and human activities throughout this century, leading to increasing restrictions on its use for irrigation (Jarray et al. 2025).

Graphical methods are commonly used to classify water samples concerning irrigation quality indicators (Machiwal et al. 2018; Güler et al. 2002; Khawla and Mohamed 2020; Ncibi et al. 2023), along with statistical methods to understand the complex behavior of aquifer processes, identify the origins of contaminants, and correlate these processes with hydrochemical characteristics (Neophytides et al. 2024; Güler et al. 2012; Panagiotou et al. 2024a, b; Panagiotou, Konstantinou, Chekirbane 2024b; Güler et al. 2002).

Most traditional graphical approaches display the relative proportion of major ions and the total dissolved solid concentration in the sample; thus, these methods are usually limited to a subset of the available dataset. The Piper diagram (Piper 1944) is the most commonly used graphical method, displaying the relative concentrations of major anions and cations on two distinct trilinear diagrams. Other methods exist that are often used to classify samples, such as the Stiff pattern diagram (Stiff 1951), US Salinity Laboratory charts (Richards 1954), Wilcox diagram (Wilcox 1948), and Schoeller diagram (Schoeller 1938). Some graphical methods are designed to display a single sample (or average) per diagram (e.g., Collins bar, Stiff), whereas other methods can show the entire dataset (e.g., Wilcox, USSL, Piper). However, none of these diagrams can produce distinct groups of datasets because of the lack of objective means (e.g., dissimilarity metrics).

An alternative approach to interpret the chemical state of water samples while producing distinct hydrochemical groups is to explore statistical associations among attributes via multivariate statistical methods (Güler et al. 2012; Machiwal et al. 2018; Panagiotou et al. 2024a). Although these methods do not guarantee the identification of cause-effect patterns, they provide a compact representation of the available information and can contribute to the investigation of hydrochemical mechanisms (Güler et al. 2002). Clustering analysis (CA) is an illustrative example of a powerful statistical tool that is commonly used to classify hydrochemical information by grouping the water samples into distinct populations (Güler et al. 2002; Mirzavand and Walter 2024; Ni et al. 2024). Principal component analysis (PCA) and factor analysis (FA) are multivariate techniques that are also commonly used to detect patterns in water samples. PCA is used mainly for reducing the dimensionality of the dataset (Panagiotou et al. 2024a, b), whereas FA is often used to identify structural dependencies among the quality factors (Tziritis et al. 2024). Unlike graphical methods, these techniques can use any combination of chemical and physical attributes, whereas the efficiency and semiobjective nature of these techniques make them superior to graphical methods for grouping the sampling data based on the available information. On the other hand, graphical methods can provide valuable insights into the chemical nature of statistical groups. The spatiotemporal patterns of these attributes exhibit high heterogeneity, requiring large and high-dimensional datasets to provide estimations with sufficient accuracy beyond the sampling locations. Consequently, interpolation techniques are widely used to capture the spatial patterns and the interrelations among relevant attributes beyond the sampling locations.

In contrast to deterministic interpolation techniques, geostatistical approaches provide predictions of attributes at unsampled locations by fitting spatial models to the available data (Chilès and Delfiner 2012). Examples of these approaches are the kriging methods, which provide two outputs at any unsampled location: (i) an estimate of the unknown geochemical variable value and (ii) a measure of uncertainty regarding that estimate. These outputs can be used to define a distribution of possible values at any unsampled location; the mean of that distribution is the kriging estimate and its variance is the kriging variance. Another advantage of kriging methods is their ability to provide the best linear unbiased prediction (BLUE) of an attribute at a target location by minimizing the prediction error variance, assuming that a variogram or covariogram model is available. Consequently, kriging estimations can be used by policymakers in probabilistic decision-making. Different kriging variants have been developed, depending on the assumptions adopted regarding the expected attribute value (average) at unsampled locations. Ordinary kriging (OK) and indicator kriging (IK) are among the most widely used kriging methods in groundwater applications (Ncibi et al. 2022; Karami et al. 2018; Hu et al. 2005; Dash et al. 2010; Arslan 2012; Bradaï et al. 2016; Islam et al. 2017; Panagiotou et al. 2022a, b).

For example, Al Kuisi et al. (2009) investigated the contamination risks in the Amman-Zarqa Basin with respect to nitrate and salinity concentrations. The OK and IK methods were combined to evaluate the spatial variability in pollutants during different periods and were used to assess the

impact of anthropogenic activities on the chemical status of the groundwater system. Dash et al. (2010) applied OK to estimate the spatial patterns of groundwater depth and several chemical properties of an aquifer located in the National Capital Territory of Delhi (India). Additionally, IK was used to identify areas at high risk of pollution according to national guidelines. Arslan (2012) investigated the spatiotemporal evolution of groundwater salinity in irrigated areas, located in the Kizilirmak Delta (northern Turkey). OK showed a decreasing trend in the salinity levels, whereas indicator kriging suggested that the northernmost region of the plain is vulnerable to salinity hazards. Delbari et al. (2016) used IK to map several water quality parameters, leading to the identification of areas where sprinkler irrigation practices are expected to be efficient. On the basis of their results, the authors suggested the usefulness of integrating geostatistical tools with geographical information systems (GIS) in probabilistic decision-making for water resource management.

The objective of the present study is to assess the suitability of the Grombalia phreatic aquifer for irrigation via the combination of traditional classification diagrams and geostatistical modeling via a relatively small dataset (i.e., 20 sampling locations). OK is used to assess the spatial variability of piezometric levels and major chemical parameters, whereas IK is used to generate probability maps exceeding critical thresholds for water quality indicators according to agricultural standards. The remainder of this paper proceeds as follows: After the study area and the details of the statistical analysis are presented in the "Material and methods" section, the spatial distributions of the geochemical parameters, along with the probabilities of major quality indicators exceeding the recommended values, are discussed in the "Results and discussion" section. Conclusions are given in the "Conclusion" section.

Material and methods

Description of the study area

The Grombalia region, covering approximately 363 km^2, is situated in the southwestern part of the Cap Bon Peninsula in Tunisia (Fig. 1a). It is bordered by the Gulf of Tunis to the north, the Takelsa Syncline to the northeast, the Abderrahman Mountain and the eastern coastal plain to the east, the plain of Hammamet to the south, and the Bouchoucha and Halloufa reliefs. During the period of 1956–2005, the region experienced a semiarid to Mediterranean subhumid climate with an average annual rainfall of approximately 488 mm (Kammoun et al. 2021; Re et al. 2017), whereas the highest precipitation rates occurred between October and January (Fig. 1b). Between 2003 and 2013, the average annual temperature was approximately 18 °C, with a maximum of 28.9 °C in July and a minimum of 8.6 °C in January (INM 2014). Furthermore, the average monthly potential evapotranspiration recorded is 76.8 mm, with the lowest amount measured in January (40.7 mm) and the highest in July (134.5 mm) (INM 2014). The region is also characterized by several ephemeral rivers or wadis that collect surface runoff from the surrounding highlands and flow toward the Gulf of Tunis.

Groundwater resources in Grombalia have historically been essential for drinking water, agriculture, and industrial purposes because of their high quality. However, excessive exploitation, improper waste disposal practices, and accidental spills of hazardous chemicals have led to a worrying decline in water quantity and quality. According to the land use map (Fig. 1a), the Grombalia region is dedicated to mixed agriculture, mainly citrus and grape production. It is also known for horticulture, particularly for the production of tomatoes, strawberries, and legumes (Re et al. 2017). Additionally, the industrial sector in the region is expanding rapidly with more than 300 factories, including the agrifood, textile, and leather sectors, located in surrounding areas such as Grombalia, Soliman, Menzel Bouzelfa, Beni Khaled, and Bouargoub.

The study area is characterized by a well-developed drainage network, with streams connected to the Belli, El Melah, Bezrik, Bou Argoub, and El Bey rivers. Interestingly, this stream network serves as the primary natural resource for recharging the aquifer system within the region, functioning as an infiltration basin (Slama and Sebei 2020). Water percolates through the soil, moving from the land surface to the aquifer. This process is particularly advantageous because of the dense network of streams, abundant annual rainfall, and comparatively low yearly evapotranspiration in the studied basin. Consequently, managed aquifer recharge (MAR) schemes were installed within the study area from 1990 to 2015, involving the collection of water from dams and subsequent discharge into more than 100 infiltration basins, targeting the augmentation of groundwater reservoirs to mitigate pollution risks (Ben Saad et al. 2023; Kammoun et al. 2021), and covering the water needs of multiple sectors. The annual amount of water that is allocated for MAR is reported to reach up to 1 million cubic meters. However, the operation of the MAR scheme was suspended in 2015 (Ben Saad et al. 2023) because of damage to critical infrastructure (basins).

The geological outcrops of the study area (Fig. 2a) range from Tertiary to Quaternary (Chihi 1995). The Tertiary formations contain four units including limestone, sandstone, and clay; gritty marl; and gritty limestone and sandstone (Tlili-Zrelli et al. 2013). The Grombalia Basin is characterized as a graben filled with 500 m of fine to coarse-grained sands, clayey sands, sandstone, and abundant evaporite deposits from the Quaternary period (Ben Moussa et al.

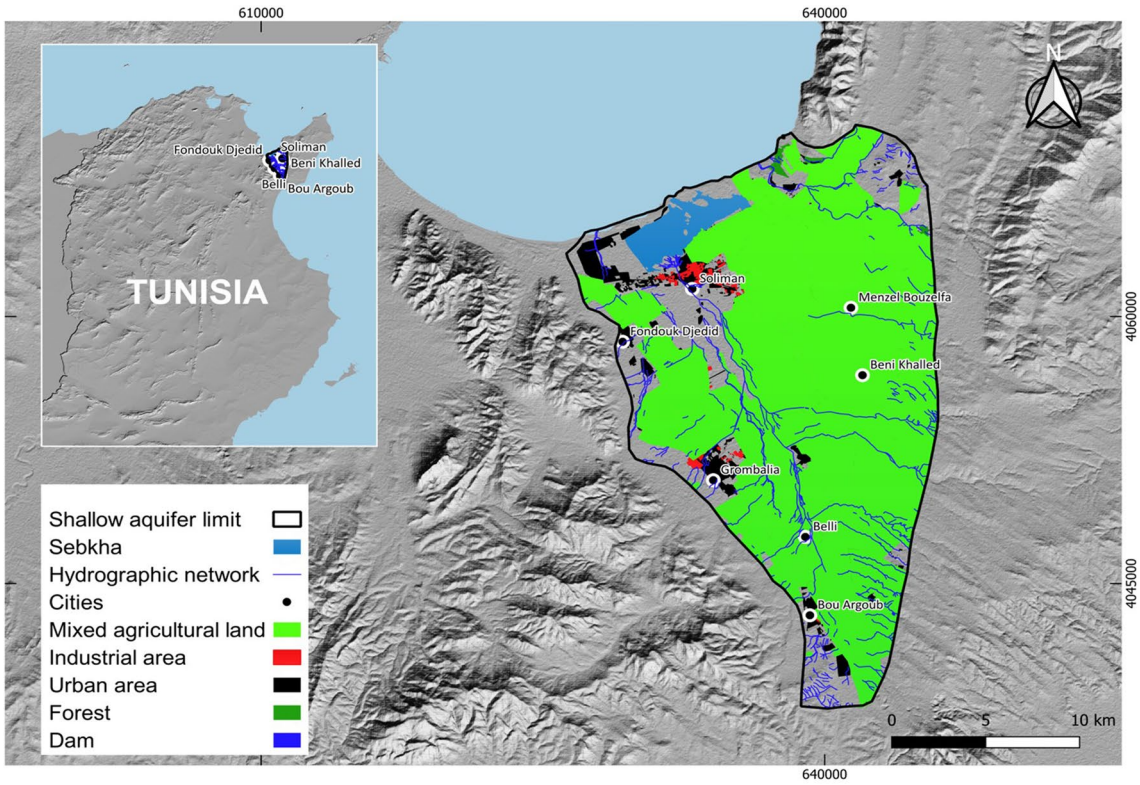

(a)

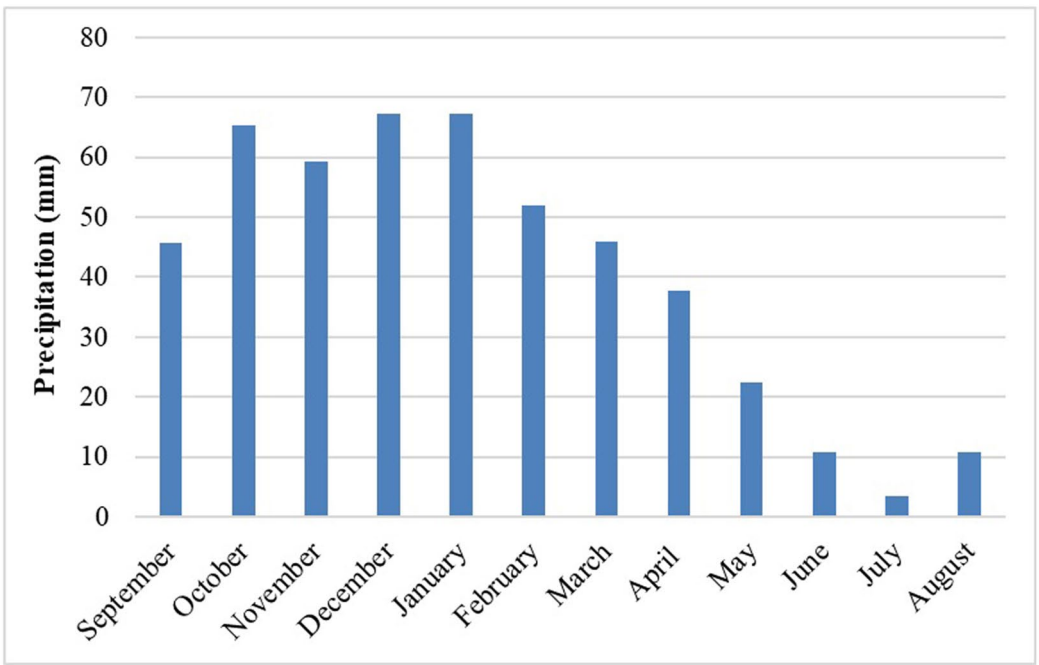

(b)

Fig. 1 **a** Land use map of the Grombalia phreatic aquifer. **b** Monthly precipitation1 rates based on measurements from nearby rainfall stations, averaged over the period 1956–2005

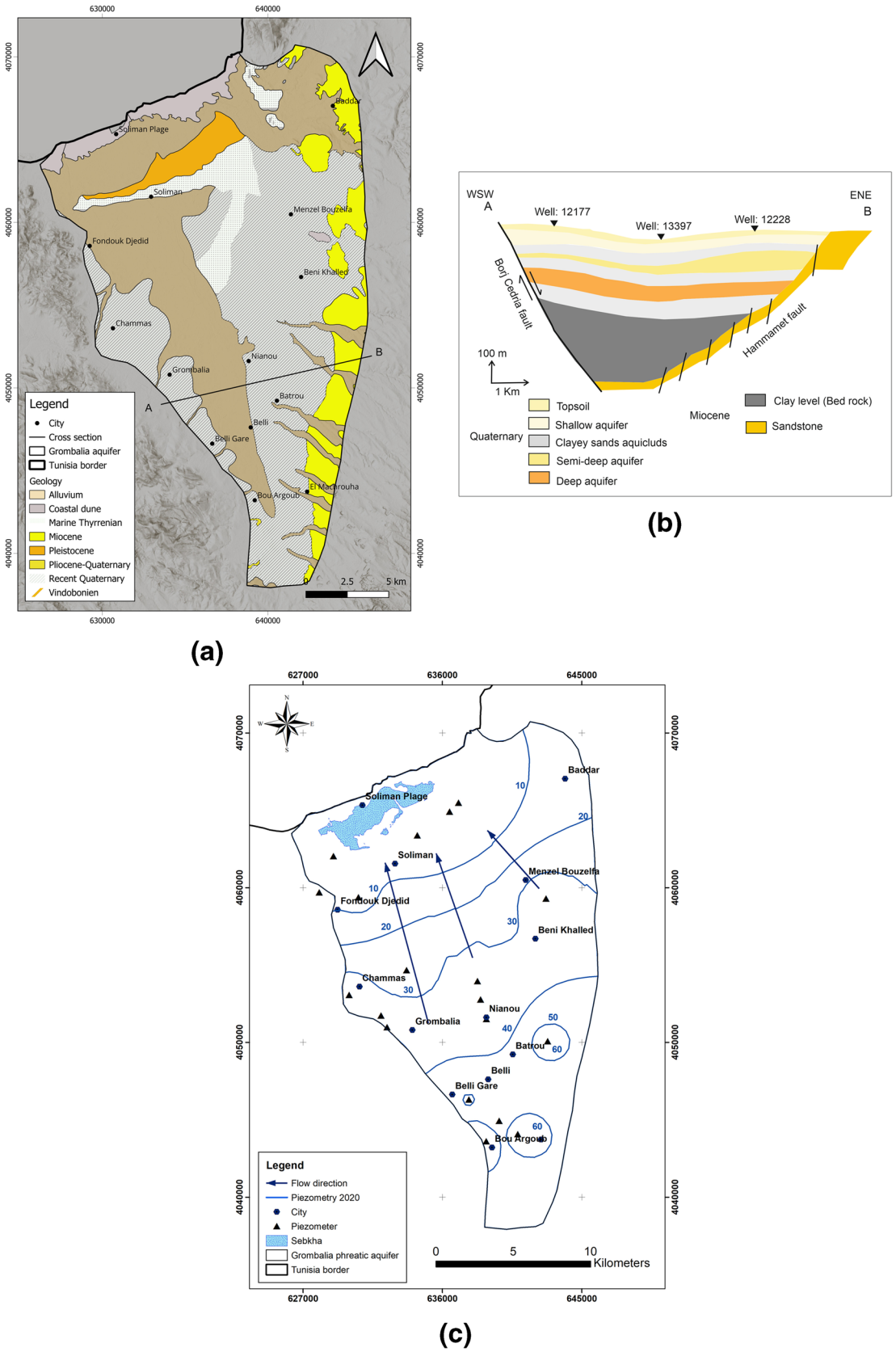

Fig. 2 **a** Geologic map of Grombalia phreatic aquifer. **b** Cross section modified (Ben Moussa et al. 2009). **c** Piezometric map of Grombalia aquifer based on data collected in 2020 (Kammoun et al. 2021)

2009; Re et al. 2017). The Quaternary sequences are primarily continental and affected by complex tectonic structures (Chihi 1995; Slama and Sebei 2020). The basin is delineated by two prominent normal faults known as the Borj Cedria NNW–SSE fault and the Hammamet NE–SW fault (Ben Moussa et al. 2009, 2010; Chihi 1995; Hadj Sassi et al. 2006), which were activated during the middle Miocene and the Quaternary (Tlili-Zrelli et al. 2013). The Beglia (Miocene) and Segui formations (Mio-Plio-Quaternary) are characterized by strong subsidence with variable depths (Chihi 1995; Hadj Sassi et al. 2006), ranging from 227 to 1000 m.

The basin comprises a multilayer aquifer system consisting of the following layers, from top to bottom: a shallow unconfined aquifer (the focus of this study) with a thickness of 50 m logged in sandstones, fine to coarse-grained sands and clayey sands of Quaternary continental deposits, an overlying confined aquifer with a thickness of 100 m, and a deep confined aquifer with a thickness of 200 m contained in Miocene sandstones (Ennabli 1980) (Fig. 2b). The shallow aquifer is recharged through pediments originating from the surrounding mountains and the central portion of the basin (Ben Moussa et al. 2010). The primary direction of groundwater flow is from southeast to northwest, flowing toward Sebkhet El Melleh (Fig. 2c) and subsequently into the Mediterranean Sea with piezometric values fluctuating from 60 m in Beni Kalled to 5 m in the Soliman region (Kammoun et al. 2021). Despite artificial recharge operations via surface infiltration basins, installed at the Mejerda–Cap Bon canal between 1990 and 2015, the piezometric level (PL) of the Grombalia aquifer, particularly in the Belli region, has generally decreased by approximately 10 m since 1972 due to overexploitation (Baccouche et al. 2024). The presence of many exploitation wells, reaching approximately 8800 in 2015, led to an increase in the exploitation rates of the shallow aquifer from 54 Mm^3/year in 1980 to 106 Mm^3/year in 2015. Over the past two decades, the Grombalia aquifer has experienced significant degradation in both water quality and quantity (Kammoun et al. 2021; Re et al. 2017).

Data collection, analytical procedures, and irrigation water quality parameters

Groundwater samples were collected from 20 shallow monitoring wells located in the Grombalia aquifer, ranging from 15 to 50 m below the ground surface (Fig. 3), during a single sampling campaign in April 2021.

All the samples were analyzed by the Wastewater and Environment Laboratory of the CERTE (LabEUE-CERTE, Tunisia). The concentration values of the measured parameters at all the sampling locations, together with the piezometric levels, are shown in the Supplementary Material (SM) (Table SM1). The analysis of physicochemical parameters was conducted simultaneously

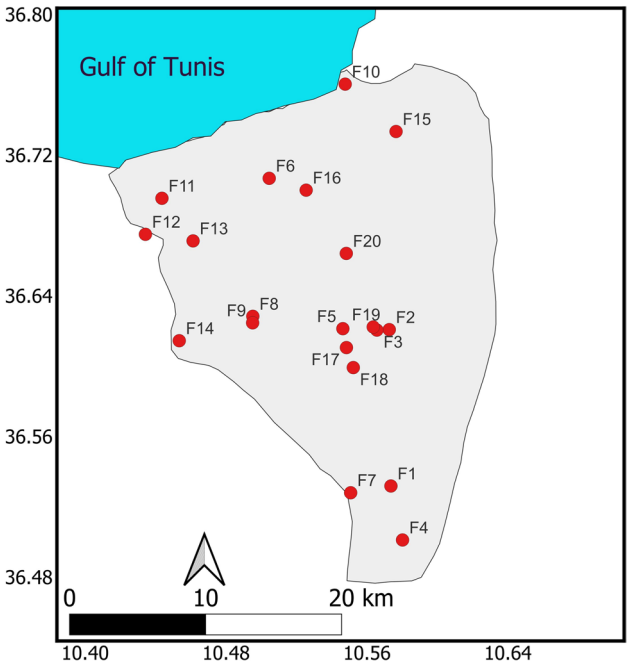

Fig. 3 Spatial distribution of the sampling locations (filled red circles) in Grombalia phreatic aquifer

via ion chromatography (940 Professional IC Vario METROHM for anions and 861 Professional IC Vario METROHM for cations), particularly for major elements Cl^-, Mg^{2+}, K^+, Ca^{2+}, NO_3^-, and Na^+, according to the standard method (ISO 10304–1:2007). The IC system was equipped with an anion-exchange column (AS4 A-SC, 150 mm × 4 mm) coupled with a conductivity detector and controlled by IC NET software. The ion standard solutions used for calibration were prepared in ultrapure water via class A volumetric glasses. The samples were filtered (0.45-µm-pore diameter membrane filters) before ionic HPLC analysis to remove particles. COD was analyzed according to the standard dichromate titrimetric method (Rodier 1975), and electrical conductivity (EC) was measured with a calibrated conductivity meter (Adwa, AD300). TDS are measured via the standard method defined by Rodier (1975).

A set of parameters was considered to assess the suitability of groundwater for irrigation. In the original work, Richards (1954) noted that the most important characteristics in determining the quality of irrigation water are the total concentration of soluble salts, the relative proportion of sodium to other cations (e.g., Ca^{2+}, $Mg^{2+}$and K^+) and the concentration of boron or other elements that may be toxic (e.g., Cl^-), and under certain conditions, the bicarbonate concentration is related to the 275 concentration of calcium plus magnesium. Several indices and chemical parameters that influence groundwater chemistry are used to investigate the suitability of groundwater for irrigation.

The first parameter is the sodium absorption ratio (SAR), which represents the relative abundance of sodium ions with respect to calcium and magnesium concentrations and is given by:

$$\mathrm{SAR} = \frac{[\mathrm{Na}^+]}{\sqrt{\frac{[\mathrm{Ca}^{2+}]+[\mathrm{Mg}^{2+}]}{2}}}, \tag{1}$$

where the subscript [.] denotes the concentration expressed in milliequivalents per liter (meq/L). A high SAR value indicates the presence of excessive sodium ions in the water, which might reduce the soil permeability and infiltration capacity. The infiltration rate increases with increasing EC for a given SAR value, and high salinity negatively affects the quantity of water available for plants (Ayers and Westcot 1985). The soluble sodium percentage (Na%) is also a widely used parameter for classifying irrigation water and is associated with the interaction of sodium with soil:

$$\mathrm{Na\%} = 100 \times \frac{\left[\mathrm{Na}^+ + \mathrm{K}^+\right]}{[\mathrm{Ca}^{2+} + \mathrm{Mg}^{2+} + \mathrm{Na}^+ + \mathrm{K}^+]}. \tag{2}$$

High values of Na% indicate low concentrations of magnesium and calcium ions, thus reducing the capacity for water movement. However, there are no universal threshold values above which the water is considered unsuitable for irrigation purposes (Ayers and Westcot 1985). Wilcox categorized irrigation water with respect to the sodium percentage as excellent if the sodium percentage is less than 20%, good if the Na% is between 20% and 40%, permissible in the 40–60% range, doubtful if it is in the 60–80% interval, and unsuitable if it is greater than 80% (Wilcox 1948). In the present study, sodium percentages less than 60% are considered permissible for irrigation on the basis of the Wilcox classification. Kelly's ratio (KR) (Kelley 1941) is used to assess the salinity levels in terms of the sodium, calcium, and magnesium concentrations in the irrigated waters, expressed as follows:

$$\mathrm{KR} = \frac{[\mathrm{Na}^+]}{[\mathrm{Ca}^{2+} + \mathrm{Mg}^{2+}]}. \tag{3}$$

KR values higher than unity indicate a surplus of sodium, thus affecting plant growth and yield, and are generally considered unsuitable for irrigation use (Hamzaoui-Azaza et al. 2020). Table 1 below lists the threshold limits for each parameter considered in this study to assess the suitability of groundwater for irrigation.

Statistical analysis

Although the Gaussian assumption is not strictly required for geostatistical estimations, a significant deviation has an adverse effect on the spatial autocorrelation of the sampling points (Goovaerts 1997; Pardo-Igúzquiza and Dowd 2005), the structural behavior of the variogram, and the reliability of the kriging estimations (Gringarten and Deutsch 2001; Ouyang et al. 2006; Varouchakis et al. 2012). Consequently, the Shapiro−Wilk test has been used to assess whether the attributes approximate a normal distribution. Logarithmic and square-root transformations were applied to mitigate the skewness of the outliers in cases where the normality assumption (p-values of the normality test are found to be less than 0.05) was not met. The resulting dataset is then used to quantify the spatial association of attribute values through structure functions, called experimental semivariograms. These functions measure how the dissimilarity of a variable evolves with the separation distance h, expressed as follows:

$$\gamma(h) = \frac{1}{2N(h)} \sum_{i=1}^{N(h)} [Z(x_i + h) - Z(x_i)]^2, \tag{4}$$

where $\gamma(h)$ is the omnidirectional experimental semivariogram, $N(h)$ denotes the number of pairwise locations separated by a distance h, and $Z(x_i)$ is the attribute value at location x_i. Fitting methods are used to model the semivariogram, allowing the prediction of variogram values for any separation distance. Three widely used semivariogram

Table 1 Threshold values for irrigation water quality parameters

Irrigation issue	Parameter	Type	Threshold limit	Guidelines	Refs
Salinity	Electric conductivity (EC) Total dissolved solids (TDS)	Value	3.0 mS/cm 2000 mg/L	FAO-UN	(Ayers and Westcot 1985)
Oxidization	Chemical oxygen demand (COD)	Value	120 mg O_2/L	Tunisian	(JORP 2018)
Toxicity	Chloride (Cl^-)	Value	700 mg L	Tunisian	(JORP 2018)
Eutrophication	Nitrate (NO_3^-)	Value	30 mg/L	FAO-UN	(Ayers and Westcot 1985)
Infiltration capacity	Sodium adsorption ratio (SAR)	Diagram	Wilcox classification	Wilcox	(Wilcox 1948)
Sodicity	Sodium percentage (Na%)	Diagram	Wilcox classification	Wilcox	(Wilcox 1948)
	Kelly's ratio (KR)	Value	1.0	Kelly	(Kelley 1941)

models, namely the spherical, exponential, and Gaussian models, are considered during the regression analysis to model the behavior of the spatial correlation structures, which are then used as inputs to kriging variants.

Ordinary kriging is the most widely used kriging variant, which assumes the existence of an unknown expected attribute value within each search neighborhood, which is different from one neighborhood to another. The ordinary kriging estimator is designed as the best linear unbiased estimator (BLUE) (Journel 1978). It is "linear" because it contains a weighted linear combination of the available data:

$$Z_{OK}(x_0) = \sum_{i=1}^{n} \lambda_{i,OK} Z(x_i), \quad \text{with} \sum_{i=1}^{n} \lambda_{i,OK} = 1 \tag{5}$$

where n denotes the total number of nearby samples contributing to the estimation at location x_0, the subscript OK denotes ordinary kriging estimation, and $\lambda_{i,OK}$ denotes the weight coefficient assigned to $Z(x_i)$ at location x_i, $I(x_i;z_k)$, which is summed to one to ensure the unbiasedness of the estimated value. Finally, the OK estimator is the best because it aims to minimize the variance of the errors (Isaaks and Srivastava 1989). More details regarding the calculation of these weights and the kriging equations can be found in relevant works (Chilès and Delfiner 2012).

Different numbers of neighboring data points are considered during the interpolation process to determine the spatial extent of the search neighborhood. The leave-one-out cross-validation process is used to evaluate the performance of the interpolation method. The deviation of the estimated values from the measured data is quantified by the root-mean-square error (RMSE), expressed as follows:

$$RMSE = \sqrt{\frac{1}{n_t} \sum_{i=1}^{n} CV_{er,i}^2}, \quad CV_{er,i} = Z_{OK}(x_i) - Z(x_i), \tag{6}$$

where n_t is the total number of samples and where $CV_{err,i}$ denotes the error obtained through the leave-one-out cross-validation process. The optimum kriging estimates for each parameter are then back-transformed to the original units of measurement. For log-transformed data, the following back-transform expressions are applied at every grid cell (Laurent 1963; Yamamoto 2007):

$$\widehat{Z}_{OK,i} = r_m \exp\left[\log_e\left(Z_{OK,i}\right) + \sigma^2_{Z_{OK,i}}\right], \tag{7}$$

where the subscript *OK,i* refers to kriging estimates at the *i*th grid cell, the hat symbol refers to the variables at the original scale of measurement, r_m is the ratio between the sample mean and the back-transformed mean, and σ denotes the standard deviation of the attribute. For square-root-transformed kriging predictions, the back-transform expression is given by the square of the kriging estimations at the unsampled locations:

$$\widehat{Z}_{OK,i} = {Z_{OK,i}}^2. \tag{8}$$

Indicator kriging (IK) refers to the application of the ordinary kriging method to estimate an indicator at a predefined threshold value, resulting in the prediction of the probability of these threshold values at locations on the basis of nearby samples. In particular, IK is a nonparametric kriging variant since it does not aim at predicting the actual attribute values but rather converts these values into binary data. The transformed dataset is then used to estimate the cumulative distribution function of an attribute at unknown locations, which is conditioned to the attribute values of the neighboring sampling points. First, the indicator variable, I, is defined via the following equation (Goovaerts 1997):

$$I(x_i;z_k) = \begin{cases} 1 \text{ if } Z(x_i) \le z_k, & k = 1, \ldots, K \\ 0 \text{ otherwise} \end{cases}, \tag{9}$$

where z_k denotes the kth cutoff and where K is the total number of cutoffs. Consequently, variogram models need to be constructed that reflect the spatial association of a particular cutoff. With respect to the empirical indicator semivariogram, $\gamma_I(h)$, every dataset of indicators at each cutoff z_k is described by the following expression:

$$\gamma_I(h) = \frac{1}{2N(h)} \sum_{i=1}^{N(h)} \left[I(x_i;z_k) - I(x_i + h;z_k)\right]^2. \tag{10}$$

Consequently, kriging estimations of the indicator variables beyond the sampling locations are obtained with the use of the IK estimator, expressed as follows:

$$Z_{IK}(x_0;z_k) = \sum_{i=1}^{n} \lambda_{i,IK} I(x_i;z_k), \tag{11}$$

where $\lambda_{i,IK}$ denotes the weight assigned to the known indicator value $I(x_i;z_k)$, which is summed to one to ensure the unbiasedness of the estimated value. More details regarding the calculation of these weights and the mathematical formulation of this kriging variant can be found in relevant works (Chilès and Delfiner 2012; Isaaks and Srivastava 1989). To represent probabilities, the kriging estimations of the water classes are bounded between zero and one and then normalized to ensure that their sum equals one at each grid cell.

In addition, different numbers of neighboring data points are considered during the interpolation process to determine the spatial extent of the search neighborhood, which is determined through a leave-one-out cross-validation process. Finally, the accuracy of the predictions is evaluated on the basis of statistical metrics (i.e., root-mean-square error, median error, median absolute deviation) of the kriging

estimations. Additionally, histograms and spatial distribution maps of the quality indicators using OK and IK are constructed to provide a comprehensive view of the degree of uncertainty, which can help the practitioners to evaluate the potential for bias and smoothing effects due to the limited sample size.

The geostatistical analysis is performed via the R programming language, particularly with the usage of *gstat* and *sf* packages (Pebesma 2004). Overall, R-4.3.2 open-source software, together with R-Studio 2023.09.1 integrated development software (IDE), was used to perform all the statistical and graphical computations.

Results and discussion

Descriptive statistics and threshold limits

The basic statistics of the groundwater quality parameters are shown in Table 2. Half of the EC concentration values exceeded the threshold limit (3 mS/cm), with the highest salinity levels measured around the Sebkha region in the northern part of the aquifer (Fig. 4). Similar mean and median values are also observed, together with weak skewness, suggesting a nearly symmetric distribution for EC. Identical patterns are observed for TDS, whereas the majority of the sampling locations (70%) are found to satisfy the quality standards.

The lowest piezometric levels are observed in the northern part of the study area, whereas the highest values are observed in the central region. Except for one, all the sampling locations exceeded the quality standards for nitrate, with the highest and lowest nitrate values occurring in the northern and southern parts of the study area respectively. With respect to chloride, most groundwater samples (65%) do not satisfy the Tunisian standards, revealing that the highest concentrations are observed in small-scale regions around hot spots located in the northern part of the study area. A strong deviation is observed between the mean and median values, thus exhibiting high skewness (2.65), whereas the maximum value of the COD data is measured in the northwestern part of the region.

As shown in Table 2, Na% values ranged from 14 to 80%, with a median of 42%, whereas all the samples (except one) presented values below 60% (permissible status for irrigation). The Wilcox diagram (Fig. 5) is used to display the combined effects of the sodium percentage and electrical conductivity on the soils and plants, revealing that only four groundwater samples (20% of the total number of wells) exist in the "Excellent-Good" and "Good-permissible" categories. Five samples (25%) are characterized as "Doubtful-Unsuitable," whereas the remaining samples belong to the "Unsuitable" area, in which the EC values exceed the threshold limit of 3 mS/cm. Overall, half of the samples were shown to be unsuitable for irrigation purposes due to high salinity levels, whereas 20% of the samples were classified as permissible.

The SAR values vary from 0.91 to 14.95 with a median of 4.64, indicating moderate skewness. The USSL diagram (Richards 1954) is also used to display the combined effects of SAR and EC on soils. In particular, the sampling dataset is partitioned into four distinct categories in terms of salinity hazard: C1 (low, EC < 0.250 mS/cm), C2 (moderate, 0.250 < EC < 0.750 mS/cm), C3 (high, 0.750 < EC < 2.250 mS/cm), and C4 (very high, EC > 2.250 mS/cm). In terms of sodium hazards, the USSL diagram is partitioned into four distinct categories: S1 (low), S2 (moderate), S3 (high), and S4 (very high). As shown in Fig. 6, the majority of the samples (55%) fall within the S2C4 class, whereas five samples (20%) fall within the high and very high sodium areas. Three samples are classified as S1C3, which are assumed to be suitable for irrigation use in the presence of good soil leaching conditions. Therefore, the majority of the samples are not suitable for irrigation use, mainly because of high salinity risks.

Table 2 Descriptive statistics of the groundwater quality parameters considered in the present study

Parameter	Minimum	Median	Mean	Maximum	Skewness	% below limit
EC (mS/cm)	0.52	3.11	3.16	6.04	− 0.004	50
TDS (mg/L)	259	1555	1580	3020	− 0.004	70
COD (mg O_2/L)	4.00	44.0	66.20	328	2.65	90
Cl^-(mg/L)	142.80	1065.35	1133.49	3323.35	1.32	35
NO_3^-(mg/L)	7.2	140.7	149.6	569.7	2.3	5
Piezo. Levels (m)	1.6	23.6	19.36	33.83	− 0.29	-
SAR (-)	0.91	4.64	5.53	14.95	1.35	-
Sodium Perce. (%)	13.92	42.34	42.54	80.07	0.78	-
KR (-)	0.15	0.72	0.84	3.51	3.30	85

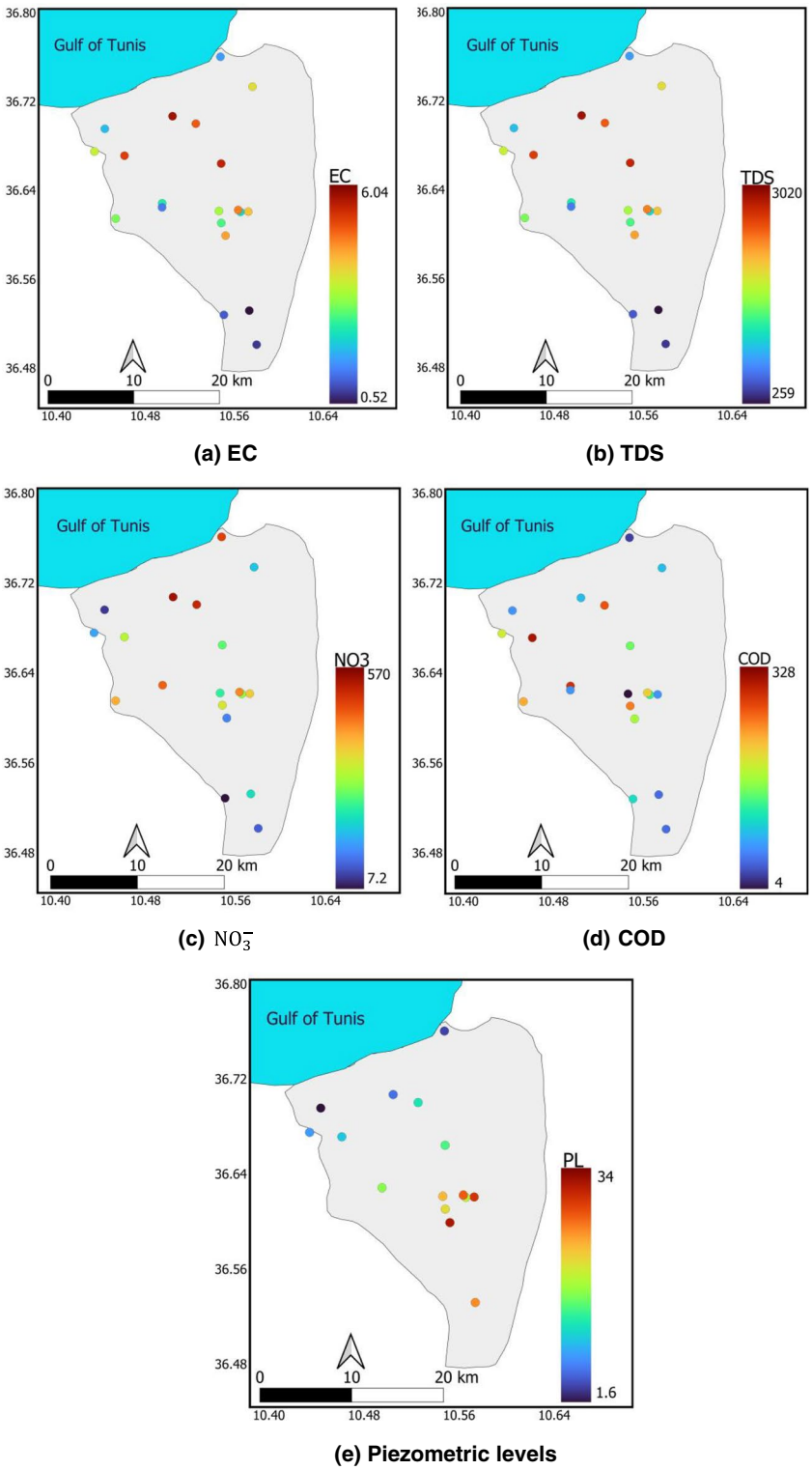

Fig. 4 Spatial distributions of electrical conductivity (mS/cm), total dissolved solids (mg/L), nitrates (mg/L), chemical oxygen demand (mg O_2/L), and piezometric levels (m) at the sampling locations

Spatial distribution of the quality parameters beyond the sampling locations via ordinary kriging

OK is used to estimate the quality parameters beyond the sampling locations. According to Shapiro−Wiki normality tests (not shown), suitable transformations are applied to both COD and Cl^- to reduce skewness and enhance normality of the distributions prior to performing the kriging estimations (Table 2).

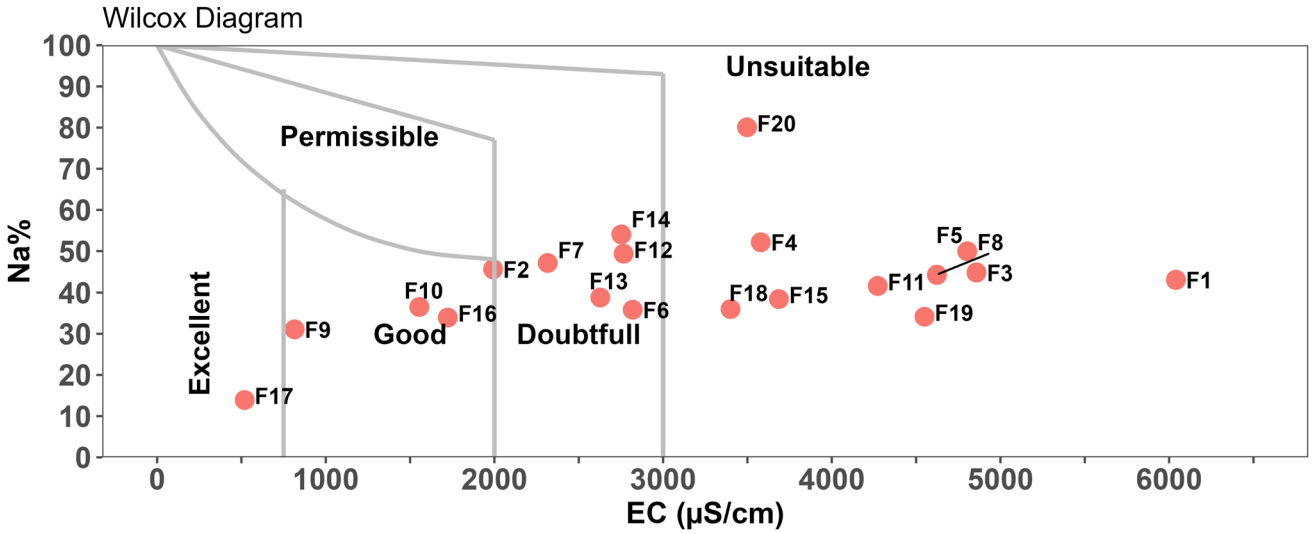

Fig. 5 Wilcox diagram for the classification of groundwater samples on the basis of the sodium percentage (Na%) and electrical conductivity (EC). Note that 1000 µS/cm is equal to 1 mS/cm

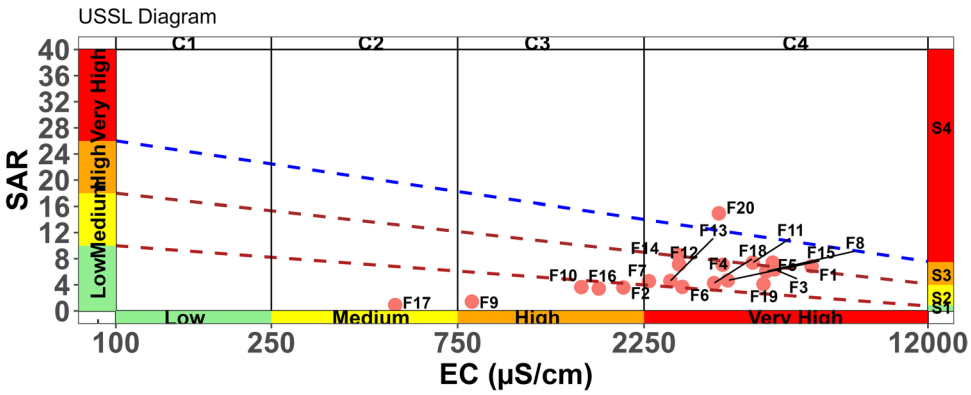

Fig. 6 USSL diagram for the classification of groundwater quality in the Grombalia phreatic aquifer in terms of SAR and electrical conductivity

Table 3 lists the types and optimized values of the fitting parameters of the variogram models, namely, the nugget, sill, and range, used for estimating the spatial distributions of the geochemical parameters, via linear regression analysis. As the table indicates, Gaussian models have been selected as the best fit for all the parameters, along with a nugget function to represent the small-scale variability of the data (Isaaks and Srivastava 1989).

Table 3 Fitting coefficients of the variogram models for four quality parameters

Parameter	Function	Nugget	Sill	Total sill	Range (m)
EC	Gaussian	0.48	2.04	2.52	6793
$\log_e$(COD)	Gaussian	0.11	1.03	1.14	3002
$\sqrt{Cl^-}$	Gaussian	1.83	134	136	1998
PL	Gaussian	4.34	36.9	41.3	3360

As described in the "Statistical analysis" section, different numbers of neighboring data points are considered during the interpolation process to determine the spatial extent of the search neighborhood (Table 4). Comparing the cross-validation errors, a minimum of 6 and a maximum of 14 nearby samples, denoted as (6,14), are used for EC, Cl^-, piezometric levels, and KR, whereas the usage of all data points in the interpolation processes, denoted as global, was found to provide the lowest errors for COD and EC.

According to Fig. 7, the highest salinity levels are observed in the central and upstream sections of the aquifer in the vicinity of the coast, whereas 36% of the total study area is expected to meet the health standards (3 mS/cm). The spatial variability of the EC reveals a discernible salinization gradient, progressing from the eastern to the western and from the southern to northern regions in the direction of Sebkhat El Maleh toward the coastal zone, which coincides with the dominant groundwater flow path according

Table 4 Cross-validation errors for different numbers of neighboring sampling points

Parameter	Numbers of neighboring sampling points (n_{min}, n_{max})		
	(4,8)	(6,14)	(1,20)
Ordinary kriging			
EC	0.94	0.83	1.13
COD	1.71	2.56	1.27
Cl^-	9.64	1.82	10.85
Piezometric levels	4.60	3.10	7.86
Indicator kriging			
EC	0.59	0.62	0.59
Kelly ratio (KR)	0.49	0.45	0.45
Chloride (Cl^-)	0.42	0.39	0.44

to the spatial extent of the piezometric levels. This observation implies a significant influence from Sebkhat El Maleh, nearby saline soils, and interactions with seawater (Slama and Sebei 2020). This salinity phenomenon can be attributed to the return of irrigated water, the substantial presence of nitrates, and the prolonged contact duration with geological formations during the water circulation (Lachaal et al. 2016).

Additionally, the high EC values could be explained by intensified agricultural activities, excessive utilization of fertilizers, the return of irrigation water, and the accumulation of stagnant water in wetland areas. Recent results of Baccouche et al. (2024) highlighted the key role that overexploitation of water resources, together with surface–groundwater interactions, play in the evolution of groundwater quantity and quality degradation in the Grombalia phreatic aquifer. Furthermore, the results of Khezami et al. (2024) indicated

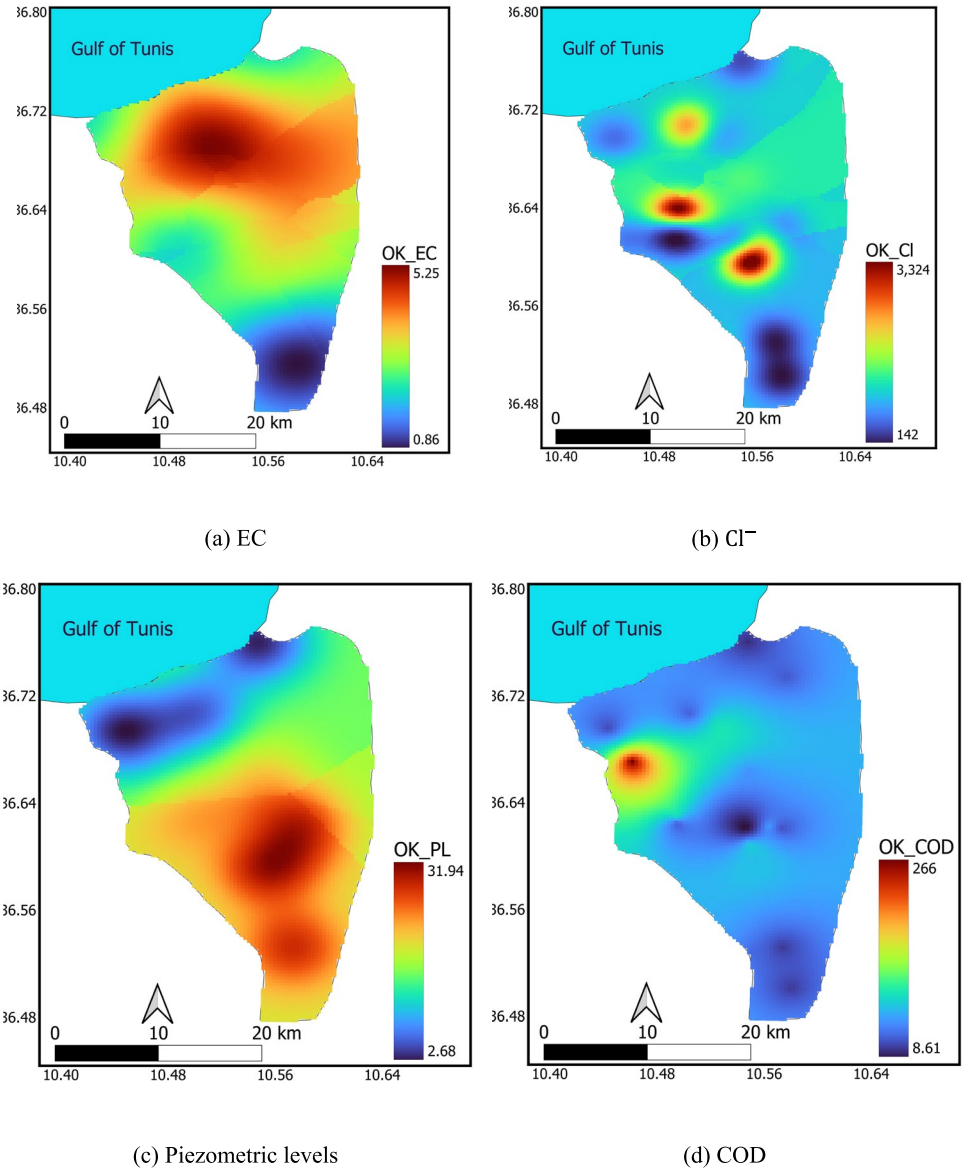

(a) EC

(b) Cl^-

(c) Piezometric levels

(d) COD

Fig. 7 Spatial distributions of **a** electrical conductivity (mS/cm), **b** chloride (Cl^-), **c** piezometric levels (m), and **d** chemical oxygen demand (mg O_2/L) with the use of ordinary kriging

that three main geochemical processes, namely, the dissolution of evaporitic formations, silicate weathering, and cation exchange, influence the evolution of groundwater chemistry in the Grombalia aquifer.

According to Slama and Sebei (2020), the dissolution process of sodium chloride (Na^+–Cl^-) is recognized as the prevailing mechanism within the Grombalia aquifer. Thus, the presence of higher chloride (Cl^-) concentrations can be attributed mainly to either the occurrence of base exchange phenomena or contamination resulting from human activities (Boughariou et al. 2018; Hamzaoui-Azaza et al. 2020; Slama and Sebei 2020; Tlili-Zrelli et al. 2013).

The enrichment of water with sodium (Na^+) can be partly attributed to the displacement of sodium from absorbed complexes in rocks and soil by calcium (Ca^{2+}) and magnesium (Mg^{2+}) ions. This process contributes to an increased concentration of Na^+ in the water. Additionally, the presence of high concentrations of chloride (Cl^-) and sodium ions (Na^+) in water can lead to increased water corrosiveness and a salty taste. The origins of Na^+ and Cl^- ions may be connected, potentially associated with the dissolution of halite (Ben Moussa et al. 2009).

The elevated concentration of COD in the northwestern section of the aquifer could be attributed to pollution transfer due to anthropogenic activities in the area. These activities include industrial and urban effluents discharge into natural water media (rivers) and agricultural runoff. According to Slama and Sebei (2020), the proximity of this zone to the industrial area of Soliman, mixed agricultural lands, and its proximity to Sebkha (salt lake) and streams contributes to the increasing levels of organic pollutants in the region. Overall, the large majority of the study area, (close to 94%) is expected to meet health standards (120 mg O_2/L).

Interestingly, low chloride values and moderate salinity levels are observed in the northeastern part of the aquifer close to the sea, as a result of the sampling data collected from a nearby well.

Finally, Table SM2 summarizes the error analysis of the kriging estimations for both OK and IK, which is needed to assess the degree of accuracy of the predicted maps. Additionally, the histograms of the OK predictions are shown in Fig. SM1, whereas the spatial variation of the kriging variance of these predictions is shown in Fig. SM2.

Identification of suitable regions for irrigation via indicator kriging

Next, IK is applied to identify regions with a high probability that the quality parameters will exceed the agricultural standards. Table 5 shows the fitted parameters of the indicator variogram models for each quality parameter. Only exponential and spherical models are considered in the fitting analysis to ensure that the linear increments of the indicator variogram model are satisfied (Dubrule 2017). Spherical functions are selected as the best fit for all irrigation parameters, with zero nuggets and ranges exceeding 5000 m.

Table 5 Details of the indicator variogram model of the three quality indicators

Parameter	Function	Nugget	Sill	Total sill	Range (m)
EC/Na%	Exponential	0.0	0.41	0.41	4979
KR	Spherical	0.0	0.17	0.17	5508
Cl^-	Spherical	0.0	0.19	0.19	5557

The resulting variogram models were used to generate probabilistic maps for the irrigation suitability parameters (Fig. 8), allowing the identification of regions that are expected to satisfy the irrigation standards. Compared with the cross-validation errors, a minimum of 6 and a maximum of 14 nearby samples are selected for all the attributes.

In accordance with the kriging estimations, the majority of the central and northern regions of the study area are not expected to satisfy the irrigation standards because of the high EC values, whereas the eastern region has high probabilities of being suitable for irrigation use. In particular, 38% of the study area is expected to be suitable for irrigation use concerning salinity, particularly EC and TDS.

Additionally, IK estimations for Cl^- reveal the dominance of low probabilities in the central and northern parts of the domain, except for small-scale coherent regions of high probabilities that exist close to the coastal interface. In contrast, a large portion of the southern part satisfies the threshold limits. As a result, most of the study area is expected to be unsuitable for irrigation in terms of this parameter (approximately 84%). This observation can be attributed to the influx of irrigation water, as the majority of the region consists of an irrigated perimeter with intensive agricultural practices. The entire study area is expected to satisfy the irrigation standards in terms of the KR, except for three isolated regions of low probability that exist in the upper region due to the presence of isolated sampling points, which are expected to exceed the threshold limits. The histograms (Fig. SM3) and the spatial variation of the quality indicators (Fig. SM4) are provided in the Supplementary Material, which can provide a comprehensive view of the uncertainty levels.

Limitations and future recommendations

Inevitably, the present study and other relevant works which are conducted in data-scarce environments are limited by the small size of the available datasets. This limitation hinders the use of advanced statistical methods and may lead to significant biases in the statistical outcomes (e.g., high cross-validation errors of the interpolation methods and high uncertainties beyond the sampling locations). In this

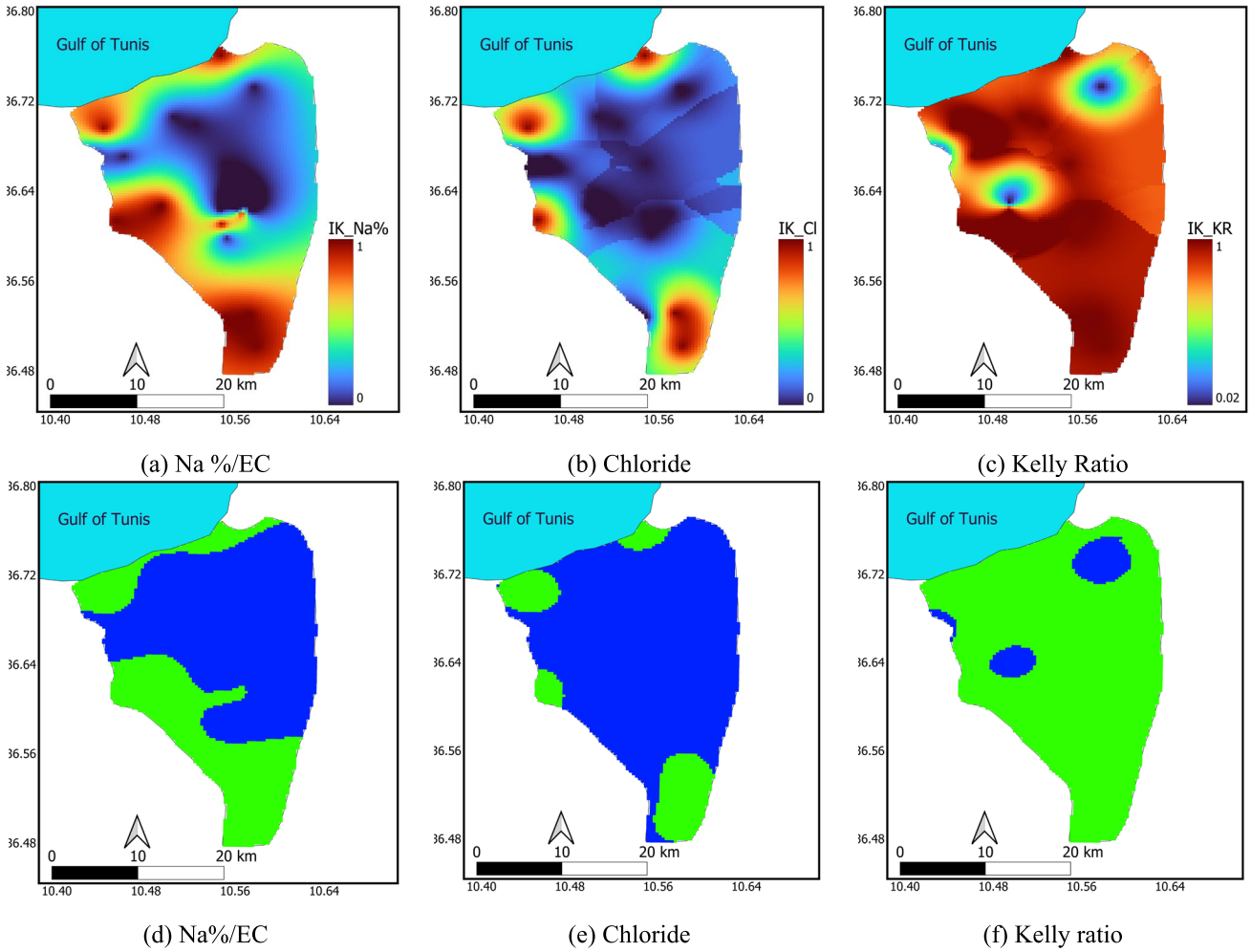

Fig. 8 Spatial distributions of the probabilities of the sodium percentage, chloride, and Kelly ratio, used to satisfy the agricultural standards shown in Table 1 (top) and the classification of groundwater quality into suitable (green area) and unsuitable (blue area) for irrigation use on the basis of the probability map (bottom)

study, the optimized values of the fitting parameters for the variogram model, as well as the number of neighboring data points that are used to predict the expected values of the attributes and build local models of spatial uncertainty, are carefully selected among several alternatives. Nevertheless, these predictions can serve as a starting point for the authorities toward the development of a cost-effective monitoring program in this area of interest. Given the availability of sufficiently large datasets, more advanced geostatistical methods can be used. For example, cokriging methods incorporate information regarding the interaction between correlated attributes into the prediction process, which can lead to improved results, whereas geostatistical simulations can "generate multiple realizations of the attribute of interest reproducing short-scale attribute variability" (Busico et al. 2024; Panagiotou et al. 2022a). Simplicial indicator kriging (Tolosana-Delgado et al. 2008) is a spatial interpolation technique that can be used to generate probabilistic maps of the attributes on the basis of specific cutoffs since it avoids the standard drawbacks of indicator kriging, such as negative probabilities, probabilities greater than one, or the occurrence of nonmonotonic conditional cumulative distribution function. Additionally, the integration of graphical and multivariate statistical methods is recommended since it can offer a framework that retains the advantages while minimizing the weaknesses of these methods.

Conclusion

The present study investigated the suitability status of the Grombalia phreatic aquifer for irrigation via the integration of kriging variants. Predictions beyond the sampling locations are obtained for major irrigation quality parameters, namely EC, Cl^-, COD, and KR, along with

piezometric levels, which are used to assess the suitability of groundwater for irrigation use. Classification on the basis of the Wilcox and USSL diagrams revealed that approximately half of the samples are unsuitable for irrigation purposes because of their high salinity levels, whereas 20% of the samples are classified as permissible.

Except for the EC and piezometric levels, suitable transformations are applied to the Cl^- and COD data, resulting in the mitigation of the impact of skewness and outliers prior to performing kriging estimations. OK is applied to the sampling data to assess the spatial distribution of the quality parameters. The spatial patterns of the EC are suggested to be highly correlated with the groundwater gradient and the spatial distribution of the piezometric levels. The greater part of the study area exceeds the recommended concentration values for Cl^-, especially around a few sampling points located in the upper part of the aquifer. A small-scale coherent region of high COD concentrations is observed in the northwestern part of the aquifer and is associated with existing industrial activities. Low chloride values and moderate salinity levels are observed in the northeastern part of the aquifer as a result of the measured data at a nearby well.

IK is used to generate probability maps for three irrigation suitability parameters, namely, the sodium percentage, chloride concentration, and Kelly ratio. The results suggest that the majority of the northern part is highly vulnerable to both salinity and toxicity hazards. For example, approximately 84% of the study area is expected to be unsuitable for irrigation with respect to chloride. Thus, the use of groundwater for irrigation in these areas is not recommended since it is expected to damage crops and reduce yield. IK estimations suggest low probabilities of exceeding the threshold limits in the southern part for all irrigation indicators, supporting groundwater use for irrigation purposes. Overall, the combination of ordinary kriging and indicator maps can assist local authorities and stakeholders in identifying suitable regions for irrigation use in terms of quality parameters at unknown locations, providing insights for future research and assisting in the design of cost-effective monitoring practices in data-scarce environments.

Supplementary information The online version contains supplementary material available at https://doi.org/10.1007/s11356-025-36512-2.

Acknowledgements The authors acknowledge the "EXCELSIOR": ERATOSTHENES: EXcellence Research Centre for Earth Surveillance and Space-Based Monitoring of the Environment H2020 Widespread Teaming project (www.excelsior2020.eu). The "EXCELSIOR" project has received funding from the European Union's Horizon 2020 research and innovation program, from the Government of the Republic of Cyprus through the Directorate General for the European Programmes, Coordination and Development and the Cyprus University of Technology. This work is also supported by the Tunisian Ministry of Higher Education and Scientific Research as part of a Tunisian national project and the PRIMA program, project InTheMED, as well as AGREEMAR PRIMA program. The PRIMA projects are supported under Horizon 2020 by the European Union's Framework for Research and Innovation.

Author contribution *Constantinos F. Panagiotou*: conceptualization, investigation, methodology, software, writing—review and editing, supervision. *Thuraya Mellah*: investigation, validation, writing, review, and editing. *Hatem Baccouche*: investigation, writing—review and editing. *Marinos Eliades*: writing—review and editing. *Lobna Mansouri*: review. *Marinos Stylianou*: writing—review and editing. *Nikos Stathopoulos*: writing—review and editing. *Hanen Jarray*: investigation, writing, review, and editing. *Hanene Akrout*: conceptualization, investigation, supervision.

Funding This study was supported by the "EXCELSIOR" project (Grant No. 857510), the InTheMED PRIMA project (Grant No. 1923), and the AGREEMAR PRIMA project (Grant No.0321/0024).

Data availability Available upon reasonable request.

Code availability Available upon reasonable request.

Declarations

Ethical approval We verify that the current manuscript presents part of the work done within the frame of the EXCELSIOR project and PRIMA InTheMED project.

Consent to participate and publish We provide consent to participate and publish our work, which is jointly contributed by all the authors.

Competing interests The authors declare no competing interests.

References

Al Kuisi M, Al-Qinna M, Margane A, Aljazzar T (2009) Spatial assessment of salinity and nitrate pollution in Amman Zarqa Basin: a case study. Environ Earth Sci 59(1):117–129. https://doi.org/10.1007/s12665-009-0010-z

Amwele HR, Kgabi NA, Kandjibi LI (2021) Sustainability of groundwater for irrigation purposes in semi-arid parts of Namibia. Front Water 3:767496. https://doi.org/10.3389/frwa.2021.767496

Arslan H (2012) Spatial and temporal mapping of groundwater salinity using ordinary kriging and indicator kriging: the case of Bafra

Plain, Turkey. Agric Water Manag 113:57–63. https://doi.org/10.1016/j.agwat.2012.06.015
Ayers RS, Westcot DW (1985) Water quality for agriculture. FAO, Rome
Baccouche H, Lincker M, Akrout H, Mellah T, Armando Y, Schäfer G (2024) Quantitative groundwater modelling under data scarcity: the example of the Wadi El Bey coastal aquifer (Tunisia). Water 16(4):522. https://doi.org/10.3390/w16040522
Ben Moussa A, Zouari K, Oueslati N (2009) Geochemical study of groundwater mineralization in the Grombalia shallow aquifer, north-eastern Tunisia: implication of irrigation and industrial waste water accounting. Environ Geol 58(3):555–566. https://doi.org/10.1007/s00254-008-1530-7
Ben Moussa A, Bel Haj Salem S, Zouari K, Jlassi F (2010) Hydrochemical and isotopic investigation of the groundwater composition of an alluvial aquifer, Cap Bon Peninsula, Tunisia. Carbonates Evaporites 25(3):161–176. https://doi.org/10.1007/s13146-010-0020-7
Ben Saad E, Ben Alaya M, Taupin JD, Patris N, Chaabane N, Souissi R (2023) A hydrogeological conceptual model refines the behavior of a Mediterranean coastal aquifer system: a key to sustainable groundwater management (Grombalia, NE Tunisia). Hydrology 10(9):180. https://doi.org/10.3390/hydrology10090180
Besbes M, Chahed J, Hamdane A (2014) Sécurité hydrique de la Tunisie. Gérer l'eau en. L'Harmattan, Paris
Boughariou E, Bahloul M, Jmal I, Allouche N, Makni J, Khanfir H, Bouri S (2018) Hydrochemical and statistical studies of the groundwater salinization combined with MODPATH numerical model: case of the Sfax coastal aquifer, Southeast Tunisia. Arabian J Geosci 11(4):69. https://doi.org/10.1007/s12517-018-3408-7
Bradaï A, Douaoui A, Bettahar N, Yahiaoui I (2016) Improving the prediction accuracy of groundwater salinity mapping using indicator kriging method. J Irrig Drain 142(7):04016023. https://doi.org/10.1061/(ASCE)IR.1943-4774.0001019
Busico G, Bordbar M, Rufino F, Sarracino A, Tedesco D (2024) Assessment of NO3, As, and F background levels in groundwater bodies: a methodological review and case study utilizing sequential Gaussian simulation (SGS). Groundw Sustain Dev 26:101211. https://doi.org/10.1016/j.gsd.2024.101211
Chihi L (1995) Les fossés néogènes à quaternaires de la Tunisie et de la mer Pélagienne: une étude structurale et une signification dans le cadre géodynamique de la Méditerranée centrale. Thèse d'État. Uni. de Tunis II
Chilès JP, Delfiner P (2012) Geostatistics: modeling spatial uncertainty, 2nd ed. John Wiley & Sons Inc. https://books.google.com.cy/books/about/Geostatistics.html?id=tZl07WdjYHgC&redir_esc=y
Dash JP, Sarangi A, Singh DK (2010) Spatial variability of groundwater depth and quality parameters in the National Capital Territory of Delhi. Environ Manag 45(3):640–650. https://doi.org/10.1007/s00267-010-9436-z
Delbari M, Amiri M, Motlagh MB (2016) Assessing groundwater quality for irrigation using indicator kriging method. Appl Water Sci 6(4):371–381. https://doi.org/10.1007/s13201-014-0230-6
Dubrule O (2017) Indicator variogram models: do we have much choice? Math Geosci 49(4):441–465. https://doi.org/10.1007/s11004-017-9678-x
Ennabli M (1980) Etude hydrogéologique des aquifères du Nord-Est de la Tunisie pour une gestion intégrée des ressources en eau. Thèse de 3e cycle, Université de Nice dans Ressources en eau de Tunisie, No. 5, 1980–1981:70–74
Gasmi T, Khouni I, Ghrabi A (2016) Assessment of heavy metals pollution using multivariate statistical analysis methods in Wadi El Bey (Tunisia). Desalin Water Treat 57(46):22152–22165. https://doi.org/10.1080/19443994.2016.1147377
Goovaerts P (1997) Geostatistics for natural resources evaluation. Oxford University Press. https://doi.org/10.1017/S0016756898631502
Gringarten E, Deutsch CV (2001) Math Geol 33(4):507–534. https://doi.org/10.1023/A:1011093014141
Güler C, Thyne GD, McCray JE, Turner KA (2002) Evaluation of graphical and multivariate statistical methods for classification of water chemistry data. Hydrogeol J 10(4):455–474. https://doi.org/10.1007/s10040-002-0196-6
Güler C, Kurt MA, Alpaslan M, Akbulut C (2012) Assessment of the impact of anthropogenic activities on the groundwater hydrology and chemistry in Tarsus coastal plain (Mersin, SE Turkey) using fuzzy clustering, multivariate statistics and GIS techniques. J Hydrol 414–415:435–451. https://doi.org/10.1016/j.jhydrol.2011.11.021
Hadj Sassi M, Zouari H, Jallouli C (2006) Contribution de la gravimétrie et de la sismique réflexion pour une nouvelle interprétation géodynamique des fossés d'effondrement en Tunisie : exemple du fossé de Grombalia. CR Geosci 338(11):751–756. https://doi.org/10.1016/j.crte.2006.07.005
Hamzaoui-Azaza F, Ameur M, Chaouch R, Cheikha LB, Gueddari M, Carrillo-Rivera JJ (2020) Assessment of groundwater quality based on GIS and geochemical methods: coastal aquifer of Bouficha (North-Eastern Tunisia). J Coast Conserv 24(4):45. https://doi.org/10.1007/s11852-020-00762-8
Henia LBZ, Benzarti Z (2008) Les nappes phréatiques et les nappes 384 profondes; Atlas de l'eau :58–65
Hu K, Huang Y, Li H, Li B, Chen D, White RE (2005) Spatial variability of shallow groundwater level, electrical conductivity and nitrate concentration, and risk assessment of nitrate contamination in North China Plain. Environ Int 31(6):896–903. https://doi.org/10.1016/j.envint.2005.05.028
INM (2014) Tableaux climatiques mensuels. Institut National de la Météorologie. https://www.meteo.tn/index.php/fr/donnees-climatiques. Accessed 26 June 2024
Isaaks EH, Srivastava RM (1989) An introduction to applied geostatistics. Oxford University Press, Oxford. https://scirp.org/reference/referencespapers.aspx?referenceid=2089815
Islam AR, Md T, Ahmed N, Bodrud-Doza Md, Chu R (2017) Characterizing groundwater quality ranks for drinking purposes in Sylhet district, Bangladesh, using entropy method, spatial autocorrelation index, and geostatistics. Environ Sci Pollut Res 24(34):26350–26374. https://doi.org/10.1007/s11356-017-0254-1
Jarray H, Mellah T, D'Oria M, Todaro V, Tanda MG, Baccouche H, Mansouri L, Ghrabi A, Akrout H (2025) Assessing pollution and water resources suitability for multiple uses under extended drought and climate change conditions: the case of the Grombalia aquifer in Tunisia. Stoch Environ Res Risk Assess 39(1):129–154. https://doi.org/10.1007/s00477-024-02854-5
JORP (2018) Par décret gouvernemental n° 2018–315 du 26 mars 2018
Journel AG, Huijbregts CJ (1978) Mining geostatistics. London Academic Press, p 600
Kammoun S, Trabelsi R, Re V, Zouari K (2021) Coastal aquifer salinization in semi-arid regions: the case of Grombalia (Tunisia). Water 13(2):129. https://doi.org/10.3390/w13020129
Karami S, Madani H, Katibeh H, Fatehi Marj A (2018) Assessment and modeling of the groundwater hydrogeochemical quality parameters via geostatistical approaches. Appl Water Sci 8(1):23. https://doi.org/10.1007/s13201-018-0641-x
Kelley WP (1941) Permissible composition and concentration of irrigation water. Trans Am Soc Civ Eng 106(1):849–855. https://doi.org/10.1061/TACEAT.0005384
Khadhar S, Mlayah A, Chekirben A, Charef A, Methammam M, Nouha S, Khemais Z (2013) Vecteur de la pollution metallique du bassin versant de l'Oued El Bey vers le Golfe de Tunis (Tunisie). Hydrol Sci J 58(8):1803–1812. https://doi.org/10.1080/02626667.2013.835487
Khawla K, Mohamed H (2020) Hydrogeochemical assessment of groundwater quality in greenhouse intensive agricultural areas in coastal zone of Tunisia: case of Teboulba region. Groundw Sustain Dev 10:100335. https://doi.org/10.1016/j.gsd.2020.100335

Khelifi F, Mokadem N, Liu G, Yousaf B, Zhou H, Ncibi K, Hamed Y (2022) Occurrence, contamination evaluation and health risks of trace metals within soil, sediments and tailings in southern Tunisia. Int J Environ Sci Technol 19(7):6127–6140. https://doi.org/10.1007/s13762-021-03531-8

Khezami F, Khiari N, Drouiche A, Chkirbene A, Zahi F, Debieche TH, Khadhar S (2024) Hydrogeochemical assessment and modeling of groundwater processes and pollution: a case study of the Grombalia aquifer in Northeast Tunisia. Model Earth Syst Environ 10(3):3573–3592. https://doi.org/10.1007/s40808-024-01968-7

Khouni I, Louhichi G, Ghrabi A (2021) Use of GIS based Inverse Distance Weighted interpolation to assess surface water quality: case of Wadi El Bey, Tunisia. Environ Technol Innov 24:101892. https://doi.org/10.1016/j.eti.2021.101892

Lachaal F, Chekirbane A, Chargui S, Sellami H, Tsujimura M, Hezzi H, Faycel J, Mlayah A (2016) Water resources management strategies and its implications on hydrodynamic and hydrochemical changes of costal groundwater: case of Grombalia shallow aquifer, NE Tunisia. J Afr Earth Sci 124:171–188. https://doi.org/10.1016/j.jafrearsci.2016.09.024

Laurent AG (1963) The lognormal distribution and the translation method: description and estimation problems. J Am Stat Assoc 58(301):231–235. https://doi.org/10.1080/01621459.1963.10500844

Machiwal D, Cloutier V, Güler C, Kazakis N (2018) A review of GIS-integrated statistical techniques for groundwater quality evaluation and protection. Environ Earth Sci 77(19):681. https://doi.org/10.1007/s12665-018-7872-x

Mirzavand M, Walter J (2024) Delineating the mechanisms controlling groundwater salinization using chemo-isotopic data and meta-heuristic clustering algorithms (case study: Saguenay-Lac-Saint-Jean region in the Canadian Shield, Quebec, Canada). Environ Sci Pollut Res 31(29):42406–42427. https://doi.org/10.1007/s11356-024-33922-6

Ncibi K, Mastrocicco M, Colombani N, Busico G, Hadji R, Hamed Y, Shuhab K (2022) Differentiating nitrate origins and fate in a semi-arid basin (Tunisia) via geostatistical analyses and groundwater modelling. Water 14(24):4124. https://doi.org/10.3390/w14244124

Ncibi K, Hamed Y, Hadji R, Busico G, Benmarce K, Missaoui R, Wederni K (2023) Hydrogeochemical characteristics and health risk assessment of potentially toxic elements in groundwater and their relationship with the ecosystem: case study in Tunisia. Environ Sci Pollut Res 30(14):40031–40048. https://doi.org/10.1007/s11356-022-25016-y

Neophytides SP, Mavrovouniotis M, Panagiotou CF, Eliades M, Chekirbane A, Hadjimitsis D (2024) Prediction of groundwater salinization using particle swarm optimization for neural network training. IGARSS 2024 - 2024 IEEE International Geoscience and Remote Sensing Symposium. pp 1927–1932. https://doi.org/10.1109/IGARSS53475.2024.10641861

Ni Q, Cao X, Zhao Z, Yuan J, Tan C (2024) An unsupervised water quality anomaly detection method based on a combination of time-frequency analysis and clustering. Environ Sci Pollut Res 31(10):15920–15931. https://doi.org/10.1007/s11356-024-32170-y

Ouyang Y, Zhang JE, Ou LT (2006) Temporal and spatial distributions of sediment total organic carbon in an estuary river. J Environ Qual 35(1):93–100. https://doi.org/10.2134/jeq2005.0221

Panagiotou CF, Kyriakidis P, Tziritis E (2022) Application of geostatistical methods to groundwater salinization problems: a review. J Hydrol 615:128566. https://doi.org/10.1016/j.jhydrol.2022.128566

Panagiotou CF, Stefan C, Papanastasiou P, Sprenger C (2022) Quantitative microbial risk assessment (QMRA) for setting health-based performance targets during soil aquifer treatment. Environ Sci Pollut Res 30(6):14424–14438. https://doi.org/10.1007/s11356-022-22729-y

Panagiotou CF, Chekirbane A, Eliades M, Papoutsa C, Akylas E, Stylianou M, Stathopoulos N (2024) Assessing the groundwater quality of El Fahs aquifer (NE Tunisia) using multivariate statistical techniques and geostatistical modeling. Appl Water Sci 14(8):170. https://doi.org/10.1007/s13201-024-02233-z

Panagiotou CF, Konstantinou C, Chekirbane A (2024) A generalized machine learning approach for cost-effective monitoring of irrigation suitability: a demonstration case in El Fahs aquifer (Tunisia). Groundw Sustain Dev 27:101324. https://doi.org/10.1016/j.gsd.2024.101324

Pardo-Igúzquiza E, Dowd PA (2005) Empirical maximum likelihood kriging: the general case. Math Geol 37(5):477–492. https://doi.org/10.1007/s11004-005-6665-4

Pebesma EJ (2004) Multivariable geostatistics in S: the gstat package. Comput Geosci 30(7):683–691. https://doi.org/10.1016/j.cageo.2004.03.012

Piper A (1944) A graphic procedure in the geochemical interpretation of water-analyses. Eos Trans Am Geophys Union 25(6):914–928. https://doi.org/10.1029/TR025i006p00914

Re V, Sacchi E, Kammoun S, Tringali C, Trabelsi R, Zouari K, Daniele S (2017) Integrated socio-hydrogeological approach to tackle nitrate contamination in groundwater resources. The case of Grombalia Basin (Tunisia). Sci Total Environ 593–594:664–676. https://doi.org/10.1016/j.scitotenv.2017.03.151

Richard LA (1954) Diagnosis and improvement of saline and alkali soils. US Department of Agriculture. Agricultural Handbook No. 60, Washington DC, 7–53. https://doi.org/10.1097/00010694-195408000-00012

Rodier J (1975) Analysis of water. Wiley, New York-Toronto

Schoeller H (1938) Notions sur la corrosion interne des canalisations d'eau. Ann Ponts Chaussées 138(2):199–282

Slama T, Sebei A (2020) Spatial and temporal analysis of shallow groundwater quality using GIS, Grombalia aquifer, Northern Tunisia. J Afr Earth Sci 170:103915. https://doi.org/10.1016/j.jafrearsci.2020.103915

Stiff HA (1951) The interpretation of chemical water analysis by means of patterns. J Pet Technol 3(10):15–23. https://doi.org/10.2118/951376-G

Taoufik G, Khouni I, Ghrabi A (2017) Assessment of physico-chemical and microbiological surface water quality using multivariate statistical techniques: a case study of the Wadi El-Bey River, Tunisia. Arab J Geosci 10(7):181. https://doi.org/10.1007/s12517-017-2898-z

Tlili-Zrelli B, Hamzaoui-Azaza F, Gueddari M, Bouhlila R (2013) Geochemistry and quality assessment of groundwater using graphical and multivariate statistical methods. A case study: Grombalia phreatic aquifer (Northeastern Tunisia). Arab J Geosci 6(9):3545–3561. https://doi.org/10.1007/s12517-012-0617-3

Tolosana-Delgado R, Pawlowsky-Glahn V, Egozcue J (2008) Simplicial indicator kriging. J China Univ Geosci 19(1):65–71. https://doi.org/10.1016/S1002-0705(08)60025-4

Tziritis E, Sachsamanoglou E, Güler C (2024) Evaluating spatiotemporal groundwater quality changes in the Rhodope coastal aquifer system (NE Greece) employing a GIS-assisted hybrid approach of multivariate statistics and inverse geochemical modeling. Sci Total Environ 947:174676. https://doi.org/10.1016/j.scitotenv.2024.174676

Varouchakis EA, Hristopulos DT, Karatzas GP (2012) Improving kriging of groundwater level data using nonlinear normalizing transformations—a field application. Hydrol Sci J 57(7):1404–1419. https://doi.org/10.1080/02626667.2012.717174

Wilcox L (1948) The quality of water for irrigation use. US Department of Agriculture, Washington DC technical bulletin no.962:1–40

Yamamoto JK (2007) On unbiased backtransform of lognormal kriging estimates. Comput Geosci 11(3):219–234. https://doi.org/10.1007/s10596-007-9046-x